



ARTICLE

Association between neuromelanin-sensitive MRI signal and psychomotor slowing in late-life depression

Kenneth Wengler^{1,2}, Brandon K. Ashinoff^{1,2}, Elena Pueraro², Clifford M. Cassidy³, Guillermo Horga^{1,2} and Bret R. Rutherford^{1,2}

Late-life depression (LLD) is a prevalent and disabling condition in older adults that is often accompanied by slowed processing and gait speed. These symptoms are related to impaired dopamine function and sometimes remedied by levodopa (L-DOPA). In this study, we recruited 33 older adults with LLD to determine the association between a proxy measure of dopamine function—neuromelanin-sensitive magnetic resonance imaging (NM-MRI)—and baseline slowing measured by the Digit Symbol test and a gait speed paradigm. In secondary analyses, we also assessed the ability of NM-MRI to predict L-DOPA treatment response in a subset of these patients ($N = 15$) who received 3 weeks of L-DOPA. We scanned a further subset of these patients ($N = 6$) with NM-MRI at baseline and after treatment to preliminarily evaluate the effects of L-DOPA treatment on the NM-MRI signal. We found that lower baseline NM-MRI correlated with slower baseline gait speed (346 of 1807 substantia nigra–ventral tegmental area (SN-VTA) voxels, $P_{\text{corrected}} = 0.038$), particularly in the more medial, anterior, and dorsal SN-VTA. Secondary analyses failed to show an association between baseline NM-MRI and treatment-related changes in gait speed, or depression severity (all $P_{\text{corrected}} > 0.361$); we however found preliminary evidence of increases in the NM-MRI signal 3 weeks post-treatment with L-DOPA compared to baseline (200 of 1807 SN-VTA voxels; $P_{\text{corrected}} = 0.046$), although the small sample size of these preliminary analyses warrants caution in their interpretation and future replications. Overall, our findings indicate that NM-MRI is sensitive to variability in gait speed in patients with LLD, suggesting this non-invasive MRI measure may provide a promising marker for dopamine-related psychomotor slowing in geriatric neuropsychiatry.

Neuropsychopharmacology (2021) 46:1233–1239; <https://doi.org/10.1038/s41386-020-00860-z>

INTRODUCTION

Late life depression (LLD) is a prevalent and disabling condition among older adults that is often recurrent, can become chronic, and is frequently non-responsive to antidepressant medication [1–4]. Motivational deficits, slowed processing speed, and gait impairments are prominent aspects of the LLD phenotype and suggest dopaminergic dysfunction may play a key pathophysiologic role [5–7]. These features are negative prognostic factors for antidepressant treatment [8] and more broadly portend adverse health outcomes, including death [9, 10]. Our recent work suggests that carbidopa/levodopa (L-DOPA) monotherapy significantly improves processing speed, gait speed, and depressive symptoms in depressed older adults by increasing dopamine availability in selected striatal subregions [11]. However, LLD is a heterogeneous and etiologically complex disorder, suggesting the need for non-invasive and scalable methods to identify dopamine-deficient individuals and personalize their treatment. As the first step in this direction, here we tested the ability of neuromelanin-sensitive magnetic resonance imaging (NM-MRI) to capture dopamine-related phenotypes in LLD, particularly psychomotor slowing.

Psychomotor slowing is of great clinical importance to LLD and has been linked to dopamine function. In LLD, decreased processing speed predicts poorer acute response to antidepressants

[8] and higher risk for dementia [12], while slowed gait increases the risk of falls [13], disability [14], and mortality [6]. Psychomotor slowing in older individuals is thought to stem at least in part from decreases in dopamine transmission with aging [15–17], consistent with human and preclinical work linking mesostriatal dopaminergic transmission to gait speed [18, 19]. Given this link, the presence of psychomotor slowing may indicate an underlying dopaminergic deficit that could be central to the pathophysiology of LLD [7], and which could possibly be remediated via pro-dopaminergic treatments such as L-DOPA. Indeed, our previous work showed that, in LLD individuals with slowed gait speed, L-DOPA monotherapy can ameliorate psychomotor slowing and depressive symptoms by normalizing mesostriatal dopamine transmission [11]. While these results are encouraging, slowed gait speed is an indirect and unspecific marker of dopamine deficits, suggesting that more direct measures like NM-MRI could optimize the selection of LLD patients who may benefit most from L-DOPA treatment.

NM-MRI is a noninvasive imaging technique that enables visualization of neuromelanin (NM) concentration in NM-rich regions [20, 21]. NM is a product of dopamine metabolism that accumulates in the dopaminergic neurons of the substantia nigra (SN) [22–25]. NM-MRI of the SN was recently validated as a marker of dopamine function, with the NM-MRI signal correlating with positron emission tomography (PET) measures of dopamine

¹Department of Psychiatry, Columbia University, New York, NY, USA; ²New York State Psychiatric Institute, New York, NY, USA and ³The University of Ottawa's Institute of Mental Health Research, affiliated with the Royal, Ottawa, ON, Canada

Correspondence: Guillermo Horga (Guillermo.Horga@nyspi.columbia.edu) or Bret R. Rutherford (brr8@cumc.columbia.edu)

These authors contributed equally: Guillermo Horga, Bret R. Rutherford.

Received: 8 May 2020 Revised: 25 August 2020 Accepted: 1 September 2020

Published online: 12 September 2020

release capacity in the striatum, and capturing dopamine dysfunctions associated with psychiatric illness [20]. NM-MRI is therefore uniquely suited as a potential biomarker for treatment selection in patients with dopamine dysfunction—including at least some LLD patients—and one that could be broadly adopted given its non-invasiveness, cost-effectiveness, and lack of ionizing radiation.

The goal of the present study was thus to determine the suitability of NM-MRI as a potential biomarker for psychomotor slowing and to begin testing its ability to predict and monitor the L-DOPA treatment response in LLD. We hypothesized that individuals with slower processing and slower gait would exhibit lower dopamine function as measured by NM-MRI. Furthermore, in a secondary analysis in a small sample, we investigated the ability of NM-MRI to predict the improvement of psychomotor slowing after L-DOPA treatment. In an exploratory analysis in a further subset of patients, we investigated the sensitivity of NM-MRI to capture longitudinal changes in dopamine function associated with L-DOPA treatment.

METHODS AND MATERIALS

Subjects

The studies described were conducted in the Adult and Late Life Depression Research Clinic at the New York State Psychiatric Institute (NYSPI) and were approved by the NYSPI Institutional Review Board. Our research program on LLD encompasses numerous therapeutic and pathophysiologic studies. In order to increase our sample size, we aggregated data from two studies having similar selection criteria and utilizing the same NM-MRI sequence. The first study ($N = 18$; Study 1) was an antidepressant treatment trial, from which we only used the baseline data. A second study ($N = 15$; Study 2) was an open-label L-DOPA trial, from which we used the baseline and post-treatment data (pre-post-L-DOPA dataset). Of these 15 individuals, we collected follow-up NM-MRI data after receiving L-DOPA in 6 subjects (Study 2 subset). See Fig. S1 for further depiction of the sample included in our analyses. All subjects ($N = 33$; Study 1 + Study 2) were adult outpatients aged ≥ 60 years who were diagnosed with Diagnostic and Statistical Manual 5 major depressive disorder, dysthymia, or depression not otherwise specified, and had a minimum depressive symptom score on a standardized scale (Hamilton Rating Scale for Depression [HRSD] ≥ 16 or Center for Epidemiologic Studies–Depression Rating Scale ≥ 10). Subjects who exhibited substance abuse or dependence, were diagnosed with a psychotic disorder, bipolar disorder, or probable dementia, had a Mini Mental Status Examination score ≤ 24 , an HRSD suicide item > 2 , or a Clinical Global Impressions–Severity score of 7 at baseline were all excluded. Subjects with an acute or severe medical illness, mobility limiting osteoarthritis or joint disease, a contraindication to MRI, or who had been treated within the past 4 weeks with psychotropic or other medications known to affect dopamine were also excluded.

Assessments

Processing speed was assessed using the Digit Symbol test from the Wechsler Adult Intelligence Scale–III [26]. Gait speed was measured in m/s as a single task in which study participants walked at their usual or normal speed on a 15-foot walking course. Two trials were completed and the final gait speed measurement was recorded as the average of these two trials. Depression severity was assessed using the 24-item HRSD.

Study 1 design

Assessments and MRI data were obtained at baseline, prior to beginning antidepressant treatment ($N = 18$). Further details can be found at <https://clinicaltrials.gov/ct2/show/NCT01931202>.

Study 2 design

Inclusion in this study also required decreased gait speed (defined as average walking speed over 15-foot course < 1 m/s). Assessments and MRI data were obtained at baseline, prior to beginning L-DOPA treatment ($N = 15$). After their MRI scan, subjects began taking 37.5 mg carbidopa/150 mg levodopa once daily (9 a.m.). After one week at this dosage, subjects were instructed to take 37.5 mg carbidopa/150 mg levodopa twice daily (9 a.m. and 5 p.m.). For the 3rd week of treatment, subjects took 37.5 mg carbidopa/150 mg levodopa three times daily (9 a.m., 12 p.m., and 5 p.m.). Participants were instructed to maintain the same timing of doses throughout the study as described above. A subset of these participants ($N = 6$) had a post-treatment MRI scan after a Week 3 visit when post-treatment assessments were performed. Please refer to the previously published main outcome manuscript for a full description of study procedures [11]; further details can be found at <https://clinicaltrials.gov/ct2/show/NCT02744391>. Processing and gait speed were assessed at baseline and then weekly during L-DOPA treatment (i.e., weeks 0–3). Assessments were performed at ~ 1 p.m. to control for time of day effects and the duration since the last morning L-DOPA dose (anticipated to be 4 h). HRSD was also performed at week 0 and week 3. Changes in processing speed, gait speed, and HRSD were taken as the difference between week 3 and week 0.

Magnetic resonance imaging

Magnetic resonance images of the brain were acquired for all participants on a GE MR750 3.0T scanner using a 32-channel phased-array Nova head-coil. NM-MRI data were acquired with a 2D gradient-recalled echo sequence with magnetization transfer contrast (2D GRE-MT) with the following parameters [20]: repetition time (TR) = 260 ms; echo time (TE) = 2.68 ms; flip angle = 40°; in-plane resolution = 0.39×0.39 mm²; partial brain coverage with field of view (FoV) = 162 mm \times 200 mm; matrix = 416 \times 512; number of slices = 10; slice thickness = 3 mm; slice gap = 0 mm; magnetization transfer frequency offset = 1200 Hz; number of excitations (NEX) = 8; acquisition time = 8.04 min. The slice-prescription protocol consisted of orienting the image stack along the anterior-commissure–posterior-commissure line and placing the top slice 3 mm below the floor of the third ventricle, viewed on a sagittal plane in the middle of the brain. This protocol provided coverage of SN-containing portions of the midbrain (and cortical and subcortical structures surrounding the brainstem) with high in-plane spatial resolution using a short scan easy to tolerate by clinical populations. For preprocessing of the NM-MRI data, a whole-brain, high-resolution T1-weighted 3D BRAVO structural MRI scan was acquired with the following parameters: inversion time = 450 ms, TR = 7.85 ms, TE = 3.10 ms, flip angle = 12°, FoV = 240 mm \times 240 mm, matrix = 300 \times 300, number of slices = 220, isotropic voxel size = 0.8 mm³).

NM-MRI data were preprocessed using a pipeline combining SPM and ANTs, previously shown to achieve high test-retest reliability [27]. The pipeline consisted of the following steps: (1) brain extraction of the T1w image using “antsBrainExtraction.sh”; (2) spatial normalization of the brain-extracted T1w image to MNI space using “antsRegistrationSyN.sh” (rigid + affine + deformable syn); (3) coregistration of the NM-MRI image to the T1w image using “antsRegistrationSyN.sh” (rigid); (4) spatial normalization of the NM-MRI images to MNI space by a single-step transformation combining the transformations estimated in steps (2) and (3) using “antsApplyTransforms”; (5) resampling of the spatially normalized NM-MRI image to 1 mm isotropic resolution using “Resample-Image”; (6) spatial smoothing of the spatially normalized NM-MRI image with a 1 mm full-width-at-half-maximum Gaussian kernel using “SPM-Smooth”. The preprocessed NM-MRI images were then used to estimate NM-MRI contrast ratio (CNR) maps. NM-MRI CNR at each voxel was calculated as the percent signal difference in NM-MRI signal intensity at a given voxel (I_v) from the

signal intensity in the crus cerebri (I_{CC}), a region of white matter tracts known to have minimal NM content as: $CNR_V = \{[I_V - \text{mode}(I_{CC})] / \text{mode}(I_{CC})\} \times 100$. Where $\text{mode}(I_{CC})$ was calculated for each participant from a kernel-smoothing-function fit of a histogram of all voxels in the CC mask [20].

Statistical analysis

Our a priori analysis tested the hypothesis that lower baseline NM-MRI CNR would correlate with slower psychomotor variables (gait speed and Digit Symbol; $N = 33$; Study 1 + Study 2). In a secondary analysis we investigated if baseline NM-MRI CNR would predict L-DOPA-induced improvements (speeding) of these psychomotor variables ($N = 15$; Study 2). These effects were tested within the substantia nigra–ventral tegmental area (SN–VTA) complex using a voxelwise analysis approach previously validated in Cassidy et al. [20]. Briefly, this method uses robust linear regression analyses and tests for significance of regression coefficients using permutation tests. The linear model used to test our a priori hypothesis (model 1) was: $CNR_V = \beta_0 + \beta_1 \cdot \text{gait speed} + \beta_2 \cdot \text{Digit Symbol score} + \beta_3 \cdot \text{HRSD} + \beta_4 \cdot \text{age} + \beta_5 \cdot \text{gender} + \beta_6 \cdot \text{education}$, with β_{1-3} being the variables of interest and β_{4-6} covariates of no-interest. The linear model for the secondary analysis (model 2) was: $CNR_V = \beta_0 + \beta_1 \cdot \Delta\text{gait speed} + \beta_2 \cdot \Delta\text{Digit Symbol score} + \beta_3 \cdot \Delta\text{HRSD} + \beta_4 \cdot \text{gait speed} + \beta_5 \cdot \text{Digit Symbol score} + \beta_6 \cdot \text{HRSD} + \beta_7 \cdot \text{age} + \beta_8 \cdot \text{gender} + \beta_9 \cdot \text{education}$, with β_{1-3} being the variables of interest and β_{4-9} covariates of no-interest. The inclusion of all variables of interest in one model provides greater specificity of effects while also providing a more conservative test that guards against false positives by adjusting the degrees of freedom in t -tests of regression coefficients [28]. The number of voxels showing a significant effect was determined to be significant through permutation testing, wherein 10,000 iterations of random permutations of the variables of interest were run while keeping the covariates of no-interest constant—see Cassidy et al. for further details [20]. This voxelwise permutation-test corrects for multiple comparisons across voxels and provides adequate protection against false positives, similar to methods used in functional-MRI studies [29].

In an exploratory analysis, we also investigated if changes in NM-MRI SN-VTA CNR can be detected after 3 weeks of L-DOPA treatment ($N = 6$; subset from Study 2). A similar voxelwise analysis approach was used, except it used a non-parametric, sign-rank test comparing pre- and post-L-DOPA treatment NM-MRI CNR values in the SN-VTA. The number of voxels showing a significant effect was determined to be significant through a permutation test in which the null distribution was derived by 10,000 iterations of random assignment of the pre- and post-L-DOPA treatment labels for each subject (i.e., 50% chance for a subject's pre-L-DOPA treatment NM-MRI CNR value to be assigned as their post-L-DOPA treatment value, with their post-L-DOPA treatment value also being assigned as their pre-L-DOPA treatment value).

A priori power analyses using effect sizes comparing baseline gait speed and dopamine function measured by PET [19] demonstrated 85% power to detect an effect in our baseline sample of 33 subjects (two-tailed, $\alpha = 0.05$) but only 50% power in our L-DOPA sample of 15 subjects. Thus, our analyses in the former sample (model 1) were sufficiently powered as our a priori test. Because of the underpowered nature of the analyses in the latter sample (model 2), they were a secondary test the results of which need to be considered preliminary. No additional corrections were implemented across a priori and secondary tests given the exploratory nature of the latter, which are presented for completeness and descriptive purposes.

To rule out potential selection bias in the follow-up NM-MRI subset from Study 2, Pearson chi-square tests or Mann–Whitney U tests were used to compare demographic and clinical characteristics between the participants in Study 2 who either received a follow-up NM-MRI scan after 3 weeks of L-DOPA treatment ($N = 6$)

and those who did not receive a follow-up NM-MRI scan after treatment ($N = 9$).

RESULTS

Sample characteristics

Clinical and demographic characteristics of the sample are provided in Table 1; for all 33 subjects, mean age was 71.8 ± 6.5 years, 63.6% were female, mean education was 16.8 ± 2.5 years, mean gait speed was 0.97 ± 0.32 m/s, mean Digit Symbol score was 36.8 ± 10.7 , and mean HRSD was 20.7 ± 6.6 . No significant differences were observed between subjects in Study 2 with a follow-up NM-MRI scan and those without a follow-up NM-MRI scan.

Baseline gait speed is associated with baseline NM-MRI

We investigated our a priori hypothesis that individuals with slower processing and those with slower gait would exhibit lower dopamine function as measured by NM-MRI in 33 patients with LLD (Study 1 + Study 2). A voxelwise linear regression model (model 1) predicted NM-MRI CNR within the SN-VTA mask as a function of gait speed, Digit Symbol score, and HRSD, with age, gender, and education as covariates. In line with our hypothesis, this revealed a set of SN-VTA voxels in which NM-MRI CNR correlated positively with gait speed (346 of 1,807 SN-VTA voxels at $P < 0.05$, robust linear regression; $P_{\text{corrected}} = 0.038$, permutation test; Fig. 1). In contrast, there was no significant effect for Digit Symbol score (194 of 1,807 SN-VTA voxels at $P < 0.05$; $P_{\text{corrected}} = 0.121$, permutation test) or HRSD (19 of 1,807 SN-VTA voxels at $P < 0.05$; $P_{\text{corrected}} = 0.731$, permutation test). A topographical analysis of the relationship between gait speed and NM-MRI CNR showed stronger relationships tended to occur in more medial ($\beta_{|x|} = 0.02$, $t_{1803} = 2.40$, $P = 0.016$), anterior ($\beta_y = 0.14$, $t_{1803} = 25.8$, $P = 10^{-124}$), and dorsal ($\beta_z = -0.05$, $t_{1803} = -6.62$, $P = 10^{-10}$) SN-VTA voxels (multiple linear regression analysis predicting the t -statistics of gait speed effect across SN-VTA voxels as a function of their coordinates in x [absolute distance from the midline], y , and z directions: omnibus $F_{3,1803} = 297$, $P = 10^{-155}$).

Secondary analyses fail to show associations between baseline NM-MRI and changes in psychomotor speed with L-DOPA treatment

In a secondary analysis, we next investigated the relationship between baseline NM-MRI signal and changes in psychomotor speed after 3 weeks of L-DOPA treatment in 15 patients with both baseline and post-treatment psychomotor evaluations (Study 2). As a more stringent and spatially constrained test of this relationship, we first determined if there was a relationship between changes in gait speed after 3 weeks of L-DOPA treatment and the average NM-MRI CNR in the 346 SN-VTA voxels that correlated positively with baseline gait speed (green voxels in Fig. 1). Here, we found no relationship between baseline NM-MRI CNR and the change in gait speed ($t_{1,9} = 0.71$, $P = 0.49$; robust linear regression testing for the effect of change in gait speed adjusting for baseline gait speed, age, gender, and education; Fig. 2). As a more lenient test of our hypothesis, we performed a voxelwise analysis in which, for each subject, we examined the relationship between changes in gait speed and Digit Symbol scores after L-DOPA treatment with baseline NM-MRI CNR within the SN-VTA mask at each voxel (model 2). Again, we found no relationship between baseline NM-MRI CNR and the change in gait speed (64 of 1,807 SN-VTA voxels at $P < 0.05$, robust linear regression testing for the effects of change in gait speed, change in Digit Symbol score, and change in HRSD adjusting for baseline gait speed, baseline Digit Symbol score, baseline HRSD age, gender, and education; $P_{\text{corrected}} = 0.377$, permutation test), change in Digit Symbol score (69 of 1,807 SN-VTA voxels at $P < 0.05$; $P_{\text{corrected}} = 0.361$, permutation test), or change in HRSD (67 of 1,807 SN-VTA voxels at $P < 0.05$; $P_{\text{corrected}} = 0.371$, permutation test).

Table 1. Demographic and clinical characteristics of the entire sample (baseline sample; Study 1 + Study 2), the subjects with pre- post-L-DOPA treatment scales (L-DOPA sample; Study 2), and the subjects with pre- and post-L-DOPA treatment NM-MRI (follow-up subgroup; Study 2 subset).

Characteristic	Baseline sample (N = 33; Study 1 + Study 2)	L-DOPA sample (N = 15; Study 2)	Follow-up subgroup (N = 6; Study 2 subset)	Test Statistic ^a	P-value ^a
Age (years)	71.8 ± 6.5	72.7 ± 6.3	73.7 ± 5.5	25.5	0.89
Sex (female)	21 (63.6%)	9 (60%)	4 (66.7%)	0.19	0.67
Education (years)	16.8 ± 2.5	16.7 ± 2.1	16.8 ± 1.8	26.0	0.98
Race					
Asian	2 (6.1%)	1 (6.7%)	0 (0.0%)	0.71	0.40
Black	12 (36.4%)	9 (60%)	3 (50.0%)	0.42	0.52
White	17 (51.5%)	4 (26.7%)	2 (33.3%)	0.23	0.63
Other	2 (6.1%)	1 (6.7%)	1 (16.7%)	1.61	0.20
Diagnosis					
MDD	26 (78.8%)	11 (73.7%)	5 (83.3%)	0.51	0.47
Dysthymia	2 (6.1%)	1 (6.7%)	0 (0.0%)	0.71	0.40
Depression NOS	5 (15.2%)	3 (20%)	1 (16.7%)	0.07	0.79
Duration of Current Depressive Episode (weeks)	634.5 ± 977.5	582.9 ± 999.7	538.0 ± 875.5	12.0	0.81
Number of Prior Antidepressant Medications	0.9 ± 1.4	0.3 ± 0.7	0.3 ± 0.5	4.5	1.00
Baseline CGI-S	3.6 ± 0.8	3.4 ± 0.8	3.3 ± 1.0	27.0	1.00
Baseline CES-D	26.5 ± 11.3	21.7 ± 11.3	20.0 ± 8.9	23.0	0.67
Baseline HRSD	20.7 ± 6.6	17.5 ± 5.8	16.5 ± 6.9	25.0	0.84
ΔHRSD	–	–7.8 ± 7.1	–5.8 ± 10.3	23.5	0.71
Baseline Digit Symbol	36.8 ± 10.7	30.0 ± 8.8	35.8 ± 10.1	10.0	0.05
ΔDigit Symbol	–	9.6 ± 8.2	7.0 ± 5.3	17.5	0.28
Baseline Gait Speed (m/s)	0.97 ± 0.10	0.77 ± 0.19	0.77 ± 0.15	24.0	0.72
ΔGait Speed (m/s)	–	0.10 ± 0.13	0.05 ± 0.10	18.0	0.29

Values are mean ± standard deviation or N (%).

CGI-S clinical global impressions–severity, CES-D center for epidemiological studies–depression, HRSD Hamilton rating scale for depression, NOS not otherwise specified.

^aComparison between subjects treated with L-DOPA with follow-up NM-MRI and those without follow-up NM-MRI.

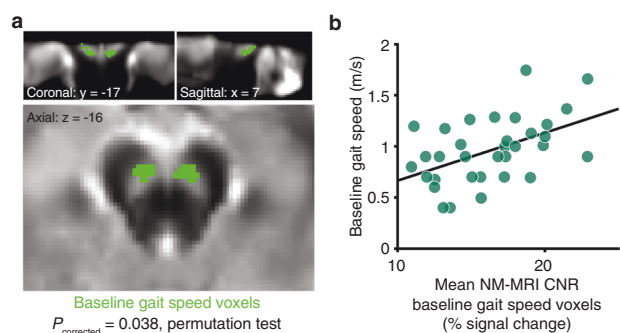


Fig. 1 Baseline NM-MRI CNR correlates with baseline gait speed. **a** Map of SN-VTA voxels where NM-MRI CNR positively correlated (thresholded at $P < 0.05$, voxel level) with a single-task measure of gait speed (green voxels) overlaid on the average NM-MRI CNR image from all subjects. **b** Scatterplot showing the average NM-MRI CNR extracted from the significant voxels in **a** plotted against gait speed for visualization purposes. These plotted data show a Pearson correlation coefficient of 0.49, although this effect-size estimate is likely inflated given the selection of significant voxels for this effect.

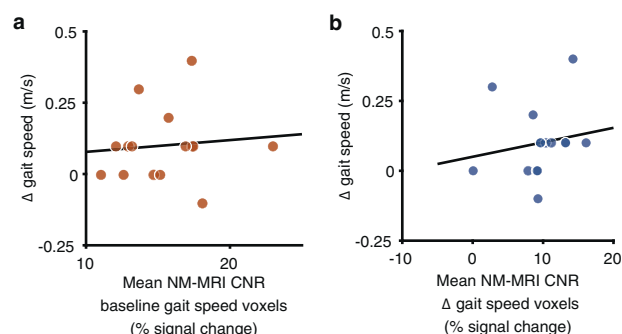


Fig. 2 Secondary analyses of baseline NM-MRI CNR do not predict changes in gait speed after 3 weeks of L-DOPA treatment in region-of-interest or voxelwise analyses. **a** Scatterplot showing the average NM-MRI CNR extracted from the significant (green) voxels in Fig. 1a plotted against gait speed. These plotted data have a Pearson correlation coefficient of 0.10. **b** Scatterplot showing the average NM-MRI CNR extracted from the voxels where NM-MRI CNR positively correlated with the change in gait speed after 3 weeks of L-DOPA treatment ($N = 64$; thresholded at $P < 0.05$, voxel level). These plotted data have a Pearson correlation coefficient of 0.17.

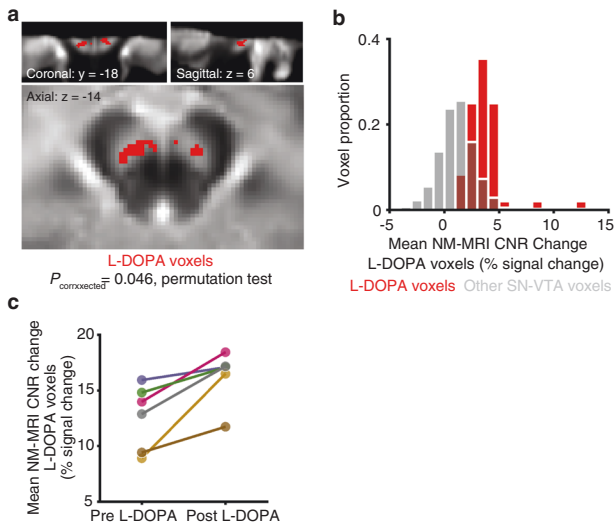


Fig. 3 NM-MRI CNR significantly increases after 3 weeks of L-DOPA treatment in an exploratory analysis. **a** Map of SN-VTA voxels where NM-MRI CNR was significantly increased after 3 weeks of L-DOPA (thresholded at $P < 0.05$, voxel level; red voxels) overlaid on the average NM-MRI CNR image from all subjects. **b** Histogram showing the average change across subjects in NM-MRI CNR after treatment including all SN-VTA voxels, which is generally shifted to the right of zero (denoting increased NM-MRI CNR). For visualization purposes, heights are proportional to either the number of L-DOPA voxels ($N = 200$; red bars corresponding to voxels in **a** or the number of Other SN-VTA Voxels (i.e., non-significant voxels; $N = 1607$); e.g., a bar with voxel proportion of 0.2 for L-DOPA voxels corresponds to 40 voxels while a bar with voxel proportion of 0.2 for Other SN-VTA Voxels corresponds to 321 voxels. **c** Ladder plot showing the average NM-MRI CNR extracted from the significant (red) voxels in **a** at baseline (Pre L-DOPA) and after 3 weeks of L-DOPA treatment (Post L-DOPA) for the 6 subjects (each shown in a different color to emphasize consistent increases across each subject).

Preliminary increases in NM-MRI CNR in the SN-VTA with L-DOPA treatment

In an exploratory analysis, we also investigated whether the NM-MRI signal changed after 3 weeks of L-DOPA treatment in the 6 patients with available baseline and post-treatment MRI data (Study 2 subset). To this end, a non-parametric voxelwise analysis was performed in which, for each subject, we tested the difference in NM-MRI CNR at baseline and post-treatment within the SN-VTA mask at each voxel. This revealed a set of SN-VTA voxels where NM-MRI CNR was significantly higher in the post-treatment scans (200 of 1,807 SN-VTA voxels at $P < 0.05$, sign-rank test testing for the difference in NM-MRI CNR at baseline and post-treatment; $P_{\text{corrected}} = 0.046$, permutation test; Fig. 3).

DISCUSSION

In this study, we investigated the relationship between NM-MRI data and psychomotor speed in older adults with LLD and found that lower NM-MRI signal in medial, anterior and dorsal parts of the SN-VTA complex was associated with slower gait speed. In a secondary analysis of a smaller sample of subjects who underwent L-DOPA treatment, we did not find that baseline NM-MRI predicted changes in psychomotor speed after treatment. Furthermore, in an exploratory analysis, we observed that 3-week L-DOPA treatment was associated with significant increases in NM-MRI signal.

Our finding of lower dopamine function, as indexed by lower NM-MRI signal, being associated with slower gait speed is consistent with our a priori hypotheses based on previous

literature [19]. For example, recent studies have identified a relationship between a genetic polymorphism of Catechol-O-methyltransferase (COMT, rs4680; which regulates tonic dopamine) and gait speed [30, 31]. Additionally, in older patients with cerebral small vessel disease, gait decline has been attributed to reductions in nigrostriatal dopamine [32]. More generally, a strong theoretical foundation implicating dopamine function of the dorsal basal ganglia in age-related motor dysfunction has been proposed [33], and supports the need for dopaminergic biomarkers in this area.

Our finding that dopamine function, as indexed by NM-MRI signal, was not associated with Digit Symbol scores was not consistent with our hypothesis or previous reports linking dopamine function and processing speed. Our limited sample size ($N = 33$) restricts our ability to conclude that there is no association between Digit Symbol scores and dopamine function, and studies in larger samples are required to address this. Dopamine is theoretically linked to processing speed [34], but empirical evidence correlating neuroimaging-based measures of dopamine signaling with performance on processing speed tasks is mixed. The largest study to date ($N = 181$ healthy adults) showed no significant correlation between striatal raclopride PET D2-receptor binding and processing speed [35]; although smaller studies have observed small, but significant, associations between processing speed and dopamine function [16, 36]. We are not aware of any studies to have demonstrated significant correlations between dopamine signaling and Digit Symbol scores specifically. Thus, while the Digit Symbol test's motor requirements and speed dependence are theoretically suggestive of a link to dopamine function, there may be greater complexity involved [37]. Furthermore, although motor speed and attention are impaired in both aging [38, 39] and depressed [40–42] populations, these deficits are often subtle and not detected through the Digit Symbol test [43]; and the mechanisms for their impairment in these clinical populations may not be dopaminergic.

In secondary analyses of our smaller sample of subjects who underwent L-DOPA treatment ($N = 15$), we failed to find an association between baseline NM-MRI and changes in psychomotor speed after treatment. This was in contrast with our hypothesis and could be due to a lack of statistical power from the small sample size. If these results hold in a larger sample size, it may suggest that baseline dopamine function is not predictive of L-DOPA efficacy regarding changes in psychomotor function.

In an exploratory analysis, we observed a significant increase in NM-MRI signal after L-DOPA treatment, supporting the notion that the L-DOPA treatment is likely increasing available striatal dopamine, but that participants are responding differently to that increase [11]. It is unlikely that the observed changes are due to natural NM accumulation over time, because this age-related process occurs very slowly and should only be detectable over a substantially longer timescale than the 3-week period evaluated here [44]. Furthermore, although our sample size is limited ($N = 6$), the excellent reproducibility of NM-MRI suggests that any observed increase in NM-MRI signal is indeed due to an increase in NM concentration [27]. Despite this result being preliminary, it provides further evidence that NM-MRI measures dopamine function, including synthesis induced by L-DOPA [45]. This result also suggests that NM-MRI may be surprisingly sensitive to changes in NM at shorter timescales than previously thought [46]. Although caution is warranted given the limitations of the sample size and further investigation is needed, if replicated in a large sample, this finding suggests that NM-MRI could be well suited for monitoring dopaminergic treatment response.

The results of our topographical analysis of the relationship between gait speed and NM-MRI signal showed that stronger relationships occurred in the medial, anterior, and dorsal areas of the SN-VTA. In contrast, NM-MRI data have shown that larger signal decreases in Parkinson's disease (PD) tend to predominate

in more lateral, posterior, and ventral voxels [20, 47]. Furthermore, histopathological studies have also found that PD-related neuron loss occurs mainly in the ventrolateral tier of the SN [48, 49], with recent free water imaging studies identifying similar spatial patterns [50, 51]. A recent study used NM-MRI to analyze the signal intensity of the SN in two motor subtypes of PD, with patients classified as either postural instability, gait difficulty dominant or tremor dominant, along with controls. Significant signal attenuation was detected in the lateral part of SN in both PD subtypes when compared with the controls, and severe signal attenuation was also observed in the medial part of SN in postural instability, gait difficulty dominant patients in comparison with the tremor dominant group [52]. Taken together, our topographical findings, in addition to the fact that slowed, depressed subjects typically do not manifest the clinical stigmata of PD (e.g., cogwheeling, freezing, tremor etc.), support that our sample of LLD patients is not likely a sample of subclinical PD patients.

Here, we used NM-MRI as a proxy marker for dopamine function and LLD-related alterations. This was supported by our previous work showing that NM-MRI captures NM concentration in ex vivo tissue samples and that it correlates with increased dopamine transmission [20]; consistent with the finding that enhancing dopamine synthesis results in increased NM accumulation [53, 54]. Although we did not hypothesize a role of NM itself in the pathophysiology of LLD, an involvement in PD has been proposed. NM is the main iron storage molecule in dopaminergic neurons of the SN and provides a neuroprotective effect by preventing the accumulation of cytosolic dopamine [53, 55]. In conditions of iron overload, NM however can play a neurotoxic role [56] and NM released into the extracellular space can cause microglial activation and subsequent neurodegeneration [57]. Given this, while we interpret our results to reflect changes in dopamine function associated with slowing and L-DOPA versus alterations in NM synthesis pathways per se, the latter possibility cannot be ruled out and should be examined in future work (e.g., combining PET dopamine and NM-MRI measures concurrently).

Some limitations of the current study are worth discussing. The open-label administration of L-DOPA in this study may have led to expectancy-based placebo effects, though some evidence suggests that these effects are diminished in older adults with depression relative to younger adults [58]. Still, a portion of the improvements observed may be attributable to these expectations, as well as to therapeutic interactions with the research staff, or to spontaneous improvement. It is plausible that we did not observe NM-MRI be predictive of treatment response because of these effects in combination with the relatively small sample size for the secondary analysis ($N = 15$). The small sample size of our study comes with an increased risk of both type I and type II errors. Although these are somewhat mitigated by using a stringent permutation test, our results should be viewed as preliminary and interpreted with caution, especially the null finding with respect to treatment response and our finding of increased NM-MRI signal in the SN-VTA after 3 weeks of L-DOPA treatment.

In conclusion, in patients with LLD, we found an association between NM-MRI signal in the SN-VTA and baseline gait speed, but not with changes in gait speed or processing speed after 3 weeks of L-DOPA treatment. Future work using a double-blind, placebo-controlled design with a larger sample is warranted to fully examine treatment effects with adequate power, to determine the relationship between NM-MRI and placebo effects, and to establish the time-course of NM-MRI signal changes under L-DOPA treatment.

FUNDING AND DISCLOSURE

We report no competing financial interest in relation to the study design, results, or discussion. GH and CMC are inventors on a

patent using the analysis method described here but have received no licensing fees or royalties. BKA received support from the NIMH (T32-MH018870). GH received funding from the NIMH (R01-MH114965 and R01-MH117323). BR received funding from the NIMH (R01-MH102293 and R61-MH110029). ClinicalTrials.gov: A Study of L-DOPA for Depression and Slowing in Older Adults; [NCT02744391](https://doi.org/10.1186/1745-7581-1-391). ClinicalTrials.gov: Mechanisms of Antidepressant Non-Response in Late-Life Depression; [NCT01931202](https://doi.org/10.1186/1745-7581-1-202).

AUTHOR CONTRIBUTIONS

KW: conceptualization, data curation, formal analysis, methodology, software, visualization, writing—original draft, writing—review and editing. BKA: methodology, writing—original draft, writing—review and editing. EP: writing—original draft, writing—review and editing. CMC: methodology, software, writing—review and editing. GH: conceptualization, funding acquisition, methodology, resources, software, supervision, writing—original draft, writing—review and editing. BRR: conceptualization, funding acquisition, investigation, methodology, resources, supervision, writing—original draft, writing—review and editing.

ADDITIONAL INFORMATION

Supplementary Information accompanies this paper at (<https://doi.org/10.1038/s41386-020-00860-z>).

Publisher's note Springer Nature remains neutral with regard to jurisdictional claims in published maps and institutional affiliations.

REFERENCES

1. Friedhoff AJ, Ballenger J, Bellack AS, Carpenter WT Jr, Chui HC, Dobrof R, et al. Diagnosis and treatment of depression in late life. *JAMA* 1992;268:1018–24.
2. Rothschild AJ. The diagnosis and treatment of late-life depression. *J Clin Psychiatry*. 1996;57:5–11.
3. Alexopoulos GS, Meyers BS, Young RC, Kakuma T, Feder M, Einhorn A, et al. Recovery in geriatric depression. *Arch Gen Psychiatry*. 1996;53:305–12.
4. Sneed JR, Rutherford BR, Rindskopf D, Lane DT, Sackeim HA, Roose SP. Design makes a difference: a meta-analysis of antidepressant response rates in placebo-controlled versus comparator trials in late-life depression. *Am J Geriatr Psychiatry*. 2008;16:65–73.
5. Sheline YI, Barch DM, Garcia K, Gersing K, Pieper C, Welsh-Bohmer K, et al. Cognitive function in late life depression: relationships to depression severity, cerebrovascular risk factors and processing speed. *Biol Psychiatry*. 2006;60:58–65.
6. Brown PJ, Roose SP, Zhang J, Wall M, Rutherford BR, Ayonayon HN, et al. Inflammation, depression, and slow gait: a high mortality phenotype in later life. *J Gerontol Ser A Biomed Sci Med Sci*. 2016;71:221–7.
7. Rutherford BR, Taylor WD, Brown PJ, Sneed JR, Roose SP. Biological aging and the future of geriatric psychiatry. *J Gerontol Ser A Biomed Sci Med Sci*. 2017;72:343–52.
8. Pimonte MA, Culang-Reinlieb ME, Morimoto SS, Sneed JR. Executive dysfunction and treatment response in late-life depression. *Int J Geriatr Psychiatry*. 2012;27:893–9.
9. Kerse N, Flicker L, Pfaff JJ, Draper B, Lautenschlager NT, Sim M, et al. Falls, depression and antidepressants in later life: a large primary care appraisal. *PLoS ONE*. 2008;3:e2423.
10. Wolinsky FD, Callahan CM, Fitzgerald JF, Johnson RJ. Changes in functional status and the risks of subsequent nursing home placement and death. *J Gerontol*. 1993;48:594–101.
11. Rutherford BR, Slifstein M, Chen C, Abi-Dargham A, Brown PJ, Wall MW, et al. Effects of L-DOPA monotherapy on psychomotor speed and [^{11}C] raclopride binding in high-risk older adults with depression. *Biol Psychiatry*. 2019;86:221–9.
12. Rapp MA, Reischies FM. Attention and executive control predict Alzheimer disease in late life: results from the Berlin Aging Study (BASE). *Am J Geriatr Psychiatry*. 2005;13:134–41.
13. Verghese J, Holtzer R, Lipton RB, Wang C. Quantitative gait markers and incident fall risk in older adults. *J Gerontol A Biol Sci Med Sci* 2009;64:896–901.
14. Guralnik JM, Ferrucci L, Pieper CF, Leveille SG, Markides KS, Ostir GV, et al. Lower extremity function and subsequent disability: consistency across studies, predictive models, and value of gait speed alone compared with the short physical performance battery. *J Gerontol A Biol Sci Med Sci*. 2000;55:M221–31.
15. Bäckman L, Nyberg L, Lindenberger U, Li S-C, Farde L. The correlative triad among aging, dopamine, and cognition: current status and future prospects. *Neurosci Biobehav Rev*. 2006;30:791–807.

16. Volkow ND, Gur RC, Wang G-J, Fowler JS, Moberg PJ, Ding Y-S, et al. Association between decline in brain dopamine activity with age and cognitive and motor impairment in healthy individuals. *Am J Psychiatr*. 1998;155:344–9.
17. Kaasinen V, Vilkman H, Hietala J, Någren K, Helenius H, Olsson H, et al. Age-related dopamine D2/D3 receptor loss in extrastriatal regions of the human brain. *Neurobiol Aging*. 2000;21:683–8.
18. Eckart C, Bunzeck N. Dopamine modulates processing speed in the human mesolimbic system. *Neuroimage* 2013;66:293–300.
19. Cham R, Studenski S, Perera S, Bohnen N. Striatal dopaminergic denervation and gait in healthy adults. *Exp Brain Res*. 2008;185:391–8.
20. Cassidy CM, Zucca FA, Girgis RR, Baker SC, Weinstein JJ, Sharp ME, et al. Neuromelanin-sensitive MRI as a noninvasive proxy measure of dopamine function in the human brain. *Proc Natl Acad Sci USA*. 2019;116:5108–17.
21. Chen X, Huddleston DE, Langley J, Ahn S, Barnum CJ, Factor SA, et al. Simultaneous imaging of locus coeruleus and substantia nigra with a quantitative neuromelanin MRI approach. *Magn Reson Imaging*. 2014;32:1301–6.
22. Zucca FA, Basso E, Cupaioli FA, Ferrari E, Sulzer D, Casella L, et al. Neuromelanin of the human substantia nigra: an update. *Neurotox Res*. 2014;25:13–23.
23. Zecca L, Shima T, Stroppolo A, Goj C, Battiston G, Gerbasi R, et al. Interaction of neuromelanin and iron in substantia nigra and other areas of human brain. *Neuroscience* 1996;73:407–15.
24. Zecca L, Bellei C, Costi P, Albertini A, Monzani E, Casella L, et al. New melanic pigments in the human brain that accumulate in aging and block environmental toxic metals. *Proc Natl Acad Sci USA* 2008;105:17567–72.
25. Sulzer D, Zecca L. Intraneuronal dopamine-quinone synthesis: a review. *Neurotox Res*. 1999;1:181–95.
26. Wechsler D. *The Wechsler Memory Scale*. San Antonio: Psychological Corp. Harcourt; 1997
27. Wengler K, He X, Abi-Dargham A, Horga G. Reproducibility assessment of neuromelanin-sensitive magnetic resonance imaging protocols for region-of-interest and voxelwise analyses. *NeuroImage* 2020;208:116457.
28. Slinker BK, Glantz SA. Multiple linear regression: accounting for multiple simultaneous determinants of a continuous dependent variable. *Circulation*. 2008;117:1732–7.
29. Eklund A, Nichols TE, Knutsson H. Cluster failure: Why fMRI inferences for spatial extent have inflated false-positive rates. *Proc Natl Acad Sci USA*. 2016;113:7900–5.
30. Hupfeld KE, Vaillancourt DE, Seidler RD. Genetic markers of dopaminergic transmission predict performance for older males but not females. *Neurobiol Aging*. 2018;66:180.
31. Rosano C, Metti AL, Rosso AL, Studenski S, Bohnen NI. Influence of striatal dopamine, cerebral small vessel disease, and other risk factors on age-related parkinsonian motor signs. *J Geront A Biol Sci Med Sci*. 2019;75:696–701.
32. Rosso AL, Bohnen NI, Launer LJ, Aizenstein HJ, Yaffe K, Rosano C. Vascular and dopaminergic contributors to mild parkinsonian signs in older adults. *Neurology*. 2018;90:e223–9.
33. Clark BC, Woods AJ, Clark LA, Criss CR, Shadmehr R, Grooms DR. The aging brain & the dorsal basal ganglia: implications for age-related limitations of mobility. *Adv Geriatr Med Res*. 2019;1:e190008.
34. Salthouse TA. Aging and measures of processing speed. *Biol Psychol*. 2000;54:35–54.
35. Nyberg L, Karalija N, Salami A, Andersson M, Wählin A, Kaboovand N, et al. Dopamine D2 receptor availability is linked to hippocampal–caudate functional connectivity and episodic memory. *Proc Natl Acad Sci USA*. 2016;113:7918–23.
36. Vriend C, van Balkom TD, van Druningen C, Klein M, van der Werf YD, Berendse HW, et al. Processing speed is related to striatal dopamine transporter availability in Parkinson's disease. *NeuroImage Clin*. 2020;26:102257.
37. Jaeger J. Digit symbol substitution test: the case for sensitivity over specificity in neuropsychological testing. *J Clin Psychopharmacol*. 2018;38:513.
38. Seidler RD, Bernard JA, Burutolu TB, Fling BW, Gordon MT, Gwin JT, et al. Motor control and aging: links to age-related brain structural, functional, and biochemical effects. *Neurosci Biobehav Rev*. 2010;34:721–33.
39. Corti EJ, Johnson AR, Riddle H, Gasson N, Kane R, Loftus AM. The relationship between executive function and fine motor control in young and older adults. *Hum Mov Sci*. 2017;51:41–50.
40. LeMoult J, Gotlib IH. Depression: a cognitive perspective. *Clin Psychol Rev*. 2019;69:51–66.
41. Li C-T, Lin C-P, Chou K-H, Chen I-Y, Hsieh J-C, Wu C-L, et al. Structural and cognitive deficits in remitting and non-remitting recurrent depression: a voxel-based morphometric study. *Neuroimage*. 2010;50:347–56.
42. Yaroslavsky I, Allard ES, Sanchez-Lopez A. Can't look away: attention control deficits predict rumination, depression symptoms and depressive affect in daily life. *J Affect Disord*. 2019;245:1061–9.
43. Shura RD, Rowland JA, Martindale SL, Brearly TW, Delahanty MB, Miskey HM. Evaluating the motor slowing hypothesis of depression. *Psychiatry Res*. 2017;252:188–95.
44. Zecca L, Fariello R, Riederer P, Sulzer D, Gatti A, Tampellini D. The absolute concentration of nigral neuromelanin, assayed by a new sensitive method, increases throughout the life and is dramatically decreased in Parkinson's disease. *FEBS Lett*. 2002;510:216–20.
45. Tison F, Mons N, Geffard M, Henry P. The metabolism of exogenous L-dopa in the brain: an immunohistochemical study of its conversion to dopamine in non-catecholaminergic cells of the rat brain. *J Neural Transm Park Dis Dement Sect*. 1991;3:27–39.
46. Matsuura K, Maeda M, Tabei K-i, Umino M, Kajikawa H, Satoh M, et al. A longitudinal study of neuromelanin-sensitive magnetic resonance imaging in Parkinson's disease. *Neurosci Lett*. 2016;633:112–7.
47. Sulzer D, Cassidy C, Horga G, Kang UJ, Fahn S, Casella L, et al. Neuromelanin detection by magnetic resonance imaging (MRI) and its promise as a biomarker for Parkinson's disease. *npj Parkinson's Dis*. 2018;4:11.
48. Damier P, Hirsch E, Agid Y, Graybiel A. The substantia nigra of the human brain: II. Patterns of loss of dopamine-containing neurons in Parkinson's disease. *Brain*. 1999;122:1437–48.
49. Fearnley JM, Lees AJ. Ageing and Parkinson's disease: substantia nigra regional selectivity. *Brain*. 1991;114:2283–301.
50. Ofori E, Pasternak O, Planetta PJ, Burciu R, Snyder A, Febo M, et al. Increased free water in the substantia nigra of Parkinson's disease: a single-site and multi-site study. *Neurobiol Aging*. 2015;36:1097–104.
51. Planetta PJ, Ofori E, Pasternak O, Burciu RG, Shukla P, DeSimone JC, et al. Free-water imaging in Parkinson's disease and atypical parkinsonism. *Brain*. 2016;139:495–508.
52. Xiang Y, Gong T, Wu J, Li J, Chen Y, Wang Y, et al. Subtypes evaluation of motor dysfunction in Parkinson's disease using neuromelanin-sensitive magnetic resonance imaging. *Neurosci Lett*. 2017;638:145–50.
53. Sulzer D, Bogulavsky J, Larsen KE, Behr G, Karatekin E, Kleinman MH, et al. Neuromelanin biosynthesis is driven by excess cytosolic catecholamines not accumulated by synaptic vesicles. *Proc Natl Acad Sci USA*. 2000;97:11869–74.
54. Cebrián C, Zucca FA, Mauri P, Steinbeck JA, Studer L, Scherzer CR, et al. MHC-I expression renders catecholaminergic neurons susceptible to T-cell-mediated degeneration. *Nat Commun*. 2014;5:3633.
55. Zucca FA, Segura-Aguilar J, Ferrari E, Muñoz P, Paris I, Sulzer D, et al. Interactions of iron, dopamine and neuromelanin pathways in brain aging and Parkinson's disease. *Prog Neurobiol*. 2017;155:96–119.
56. Zecca L, Casella L, Albertini A, Bellei C, Zucca FA, Engelen M, et al. Neuromelanin can protect against iron-mediated oxidative damage in system modeling iron overload of brain aging and Parkinson's disease. *J Neurochem*. 2008;106:1866–75.
57. Zecca L, Wilms H, Geick S, Claasen J-H, Brandenburg L-O, Holzknacht C, et al. Human neuromelanin induces neuroinflammation and neurodegeneration in the rat substantia nigra: implications for Parkinson's disease. *Acta Neuropathol*. 2008;116:47–55.
58. Rutherford BR, Wall MM, Brown PJ, Choo T-H, Wager TD, Peterson BS, et al. Patient expectancy as a mediator of placebo effects in antidepressant clinical trials. *Am J Psychiatr*. 2017;174:135–42.